Multimodal Biometrics Sensor Reliability Evaluation for Personal Identification

DIMITAR GEORGIEV
School for PhD students
Technical University of Sofia
8 Kliment Ohridski Blvd., 1756 Sofia
BULGARIA
dimitargeogiev11@gmail.com http://ff.tu-sofia.bg/

TASHO TASHEV
Electrical Measurement Systems Dept.
Technical University of Sofia
8 Kliment Ohridski Blvd., 1756 Sofia
BULGARIA
ttashev@tu-sofia.bg http://elfe.tu-sofia.bg

IVO DRAGANOV
Radio Communications and Video Technologies Dept.
Technical University of Sofia
8 Kliment Ohridski Blvd., 1756 Sofia
BULGARIA
idraganov@tu-sofia.bg http://rcvt.tu-sofia.bg

Abstract: - In this paper a prognostic analysis is made on two types of biometric sensors – optoelectronic and capacitive one. The first is capable of capturing both the human fingerprints and finger veins while the other is applicable only to fingerprints. Their reliability is found by Weibull analysis and their operation is opposed to the expected load of an air border-crossing point for a 12 years period. Useful conclusions are made for the applicability of both type of sensors in terms of their durability to operate under the ever increasing flow of passengers.

Key-Words: - capacitive sensor, optoelectronic sensor, fingerprint, finger vein, biometrics, personal identification

1 Introduction

Fingerprints are biometric feature used for personal identification on a wide scale. Fingerprint sensors, being a part of a complete fingerprint readers, allow to capture the fingerprint pattern in the form of an image digitized and ready to be further processed by computational means. There are three main groups of this kind of sensors: swipe, touch and touchless [1]. The first group capture the pattern line by line with the linear movement of the finger in parallel to the scanning element while the other two complete the process in one pass after the finger is put to their proximity. Touch and touchless sensors register patterns with a quality leading to lower False Rejection Rate (FRR) at higher price. They manage to achieve accuracy despite the fact that most often the covered area of the finger is smaller than that of swipe sensors. Capturing is also faster for them and thus pose more comfort to the user.

The basic principles on which fingerprint sensors rely on are:

- Optical – visible light is the initial carrier of the fingerprint pattern later transformed into electrical signal by photo-sensitive diodes or transistors [2]. They are built on CCD or CMOS technology. The first type assures better sensitivity to low levels of illumination and therefore better intensity resolution leading to more detailed representation of the registered prints. Initial source of the light, which reflects from the bottom part of the finger, is more often one or more light emitting diodes. CMOS sensors are currently cheaper, due to

the maturity of the manufacturing process of integrated design, and more efficient from power consumption point of view than CCD. Circuitry performing some of the processing algorithms over captured data could be embedded within a CMOS sensor chip. Optical fingerprint sensors are first to appear historically and currently are the most widely distributed. In general, they are cheap but susceptible to spoofing, with relatively large size unsuitable for mobile use, affected by contamination and aging as per their performance.

- Capacitive – an array of capacitor elements in the form of plates which hold electrical charge induced by the presence of a human finger in nearby vicinity generate the visual representation of its print corresponding to the spatial position of ridges and valleys over it [3, 4]. Spoofing is much harder to achieve without an actual finger because of the very principle of operation. Smaller size makes them proper to integrate into mobile devices. There are two types of registering the accumulated charge:
  - Passive – low or no voltage may be supplied to the finger in order to directly measure the charge from each plate. The process is based on the conductivity of the skin. Its condition (dryness, damages) may influence the quality of the resulting image as well as static discharges. No dependence by outer illumination exist but very slim coating is a must for precise measurement.
  - Active – low voltage is passed to the finger skin, e.g. by a conductive frame around the sensor, leading to its charge. Then follows discharge cycle during which accumulated charge is compared to reference levels. Local capacitance at each plate then could be calculated and from it the distances to the points from skin corresponding to ridges and valleys. These distances helps in constructing the image of the fingerprint. Adaptation to various skin conditions becomes possible by incorporation of processing units within the same integrated circuit. Contamination also has less effect on the precision for this type of sensors. Thicker covering, resistant to outer influences, also become possible to embrace the plates. The image quality is considered higher than passive sensors and much resilient to attacks. Small size, lower power consumption, fast operation and relatively low cost are another benefits from using these sensors in fingerprinting. Proper adjustment of the sensitive layer could allow liveness elicitation for enhanced security.
- Ultrasonic – sound (emitted by piezoelectric transducers) with frequencies higher than these for tones audible to humans obliterates the skin of the finger and penetrates partially into the epidermis [5]. Some of these waves reflects back to piezoelectric sensors where registration takes place and forms the fingerprint image. Contamination of outer surfaces of the device and the condition of the skin are not considerable issue. Liveness could also be detected with these sensors. Considerably dry skin could lower the level of detail of obtained images though. Also, ultrasonic sensors are slower than the above mentioned types, more expensive, consuming more power, and larger in size. They also require computationally expensive algorithms for data processing to construct the final image.
- Thermal – pyro-electric materials reacts to temperature levels so when the ridges of the finger are with contact to an array of cells made of such matter, the unique print could be captured [6]. The dependence of skin temperature variation over short periods, contaminations and abrasions become problematic to the efficiency of these sensors. If the surrounding temperature is equal to that of the finger, the sensor needs heating up in order to operate. Thermal pulses to each cell could solve some of these issues but requires more power and observed images are not that detailed.
- Pressure – mechanical stress over thin layers of matter, non-conducting from outside, reacting with an electrical signal as response when pressed by a finger produce currents proportional by amplitude to the position of the ridges and valleys on it [7]. Still, their operation depends highly on temperature variation. As benefit they have smaller sizes suitable for portable devices.

Fig. 1 depicts a comparison among all described sensor technologies on a scale from 1 to 5 in relation to 7 criteria [8].

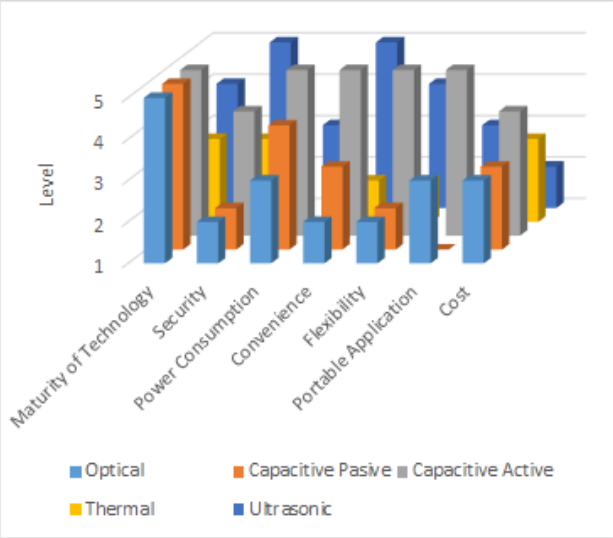

Fig. 1. Fingerprint sensor technologies comparison

Finger veins are another unique feature for every human that may be used for personal identification. It does not change considerably within lifetime, including variable health status, and being hidden within the body does not allow easy spoofing [9]. The leading principle of obtaining finger vein patterns is optical with two major design types of the sensors. The first is transmissive [10] where the finger is illuminated from the back side with near-infrared light emitting diodes and CCD or CMOS sensor on the other side captures the veins image. The other is reflective [11] – the illuminator and the sensor are below the front side where the ridges and valleys forming the fingerprint are and relying on internal reflection of the stream, combined with partial diffusion, the image is registered. The second design permits smaller size of the overall sensor structure and opportunity to combine fingerprint capturing with that of the veins. Most of the qualities of the optical fingerprint sensors, as stated above, are similar in this case. Both capturings could be done simultaneously which means at least twice reduction of the time in comparison to conventional fingerprinting is achieved. Further both biometrics could be combined, as previously proposed [12], to get higher confidence of the personal identification.

In this study an evaluation of the reliability of two of the most common types of sensors – an optical and capacitive – is undertaken. It relies on real-world use-case scenario based on the typical load of passengers at a particular border-crossing point. The first type of sensor is able to capture only fingerprints, currently used independently from face (being the main feature) and signature (almost unused) to verify travelers' identity. The second uses optoelectronic sensor to get both the fingerprint and finger veins patterns of each passenger in one scan. In Section 2 the evaluation methodology for estimating the reliability of the sensors is described followed by description of the approach to predict the traffic load of travelers which determines the stress level of operation for the sensors. Detailed structure and basic parameters for the latter are given in Section 4. Section 5 contains the reliability analysis followed by a discussion in Section 6. Then, conclusion is made in Section 7.

2 Reliability evaluation methodology

Weibull analysis [13] could provide the relative amount of biometric sensors working simultaneously from initial entity given a particular number of cycles without a failure (successful capturing operations). Let *p(c)* is the density distribution over the number of cycles *c*:

$$p(c) = g'(c)e^{-g(c)}, \quad (1)$$

where g is monotonically increasing function that holds $g(0) = 0$, $\lim_{c\to\infty} g(c) = \infty$. Then the cumulative probability function is:

$$f(c) = 1 - e^{-g(c)}. \quad (2)$$

The rate of $p(c)$ by definition is:

$$r(c) = \frac{p(c)}{1-f(c)} \quad (3)$$

and substituting (1) and (2) in (3) gives:

$$\mathrm{r(c)} = \frac{g'(c)e^{-g(c)}}{1-(1-e^{-g(c)})} = g'(c). \quad (4)$$

Knowing the rate function it becomes possible to find or define the density probability function. The Weibull distributions in general could be expressed as [14]:

$$\mathrm{r(c)} = \frac{\beta}{\alpha}\left(\frac{c}{\alpha}\right)^{\beta-1}, \quad (5)$$

where α is the characteristic life of the product, in this case a sensor, and β – shape parameter.

Integrating (5) leads to $g(c)$ of the form:

$$\mathrm{g}(c) = \left(\frac{c}{\alpha}\right)^{\beta} \quad (6)$$

and cumulative density distribution:

$$\mathrm{f(c)} = 1 - \mathrm{e}^{-\left(\frac{c}{\alpha}\right)^{\beta}}. \quad (7)$$

The density function then holds:

$$\mathrm{p(c)} = \frac{\beta}{\alpha}\left(\frac{c}{\alpha}\right)^{\beta-1} e^{-\left(\frac{c}{\alpha}\right)^{\beta}} \quad (8)$$

and the amount of failures per component expected for cycles *c* is:

$$\mathrm{F(c)} = 1 - \mathrm{e}^{-\left(\frac{c}{\alpha}\right)^{\beta}}. \quad (9)$$

Equation (9) could be transformed in the following fashion:

$$1 - \mathrm{F(c)} = \mathrm{e}^{-\left(\frac{c}{\alpha}\right)^{\beta}}, \quad (10)$$

$$\ln(1 - \mathrm{F(c)}) = -\left(\frac{c}{\alpha}\right)^{\beta}, \quad (11)$$

$$\ln\left(\frac{1}{1-\mathrm{F(c)}}\right) = \left(\frac{c}{\alpha}\right)^{\beta}, \quad (12)$$

$$\ln\left(\ln\left(\frac{1}{1-\mathrm{F(c)}}\right)\right) = \beta\ln\left(\frac{c}{\alpha}\right), \quad (13)$$

$$\ln\left(\ln\left(\frac{1}{1-\mathrm{F(c)}}\right)\right) = \beta\ln(x) - \beta\ln(\alpha). \quad (14)$$

Each component, then, could failed by the cycle c_t according to probability $P_t = f(c_t)$. Given the whole population of L elements at the very same cycle c_t it is expected to have l of them having failed and L-l continuing to operate with the following probabilities, respectively:

$$P_{tl} = \binom{L}{l} P_t^l (1 - P_t)^{L-l}, \quad (15)$$

$$P_{t(L-l)} = \sum_{k=l}^{L} \binom{L}{k} P_t^k (1 - P_t)^{L-k}. \quad (16)$$

The median value of P_t, also known as median rank, is found by selecting $P_{t(L-l)} = 0.5$. For sake of

computational complexity the approximate equation, given below, gives accurate enough results [14]:

$$f(c_t) = \frac{l-0.3}{L+0.4}. \quad (17)$$

Linear regression could give a line that fits n data points from testing by using the least-square approach. Let put $u_t = \ln(c_t)$, so:

$$w_t = ln\left[ln\left(\frac{1}{1-\frac{l-0.3}{L+0.4}}\right)\right] \quad (18)$$

and the values of the constants describing the Weibull distribution for any current case will be:

$$\beta = \frac{n\sum_{i=1}^{n} u_i w_i - (\sum_{i=1}^{n} u_i)(\sum_{i=1}^{n} w_i)}{n\sum_{i=1}^{n} u_i^2 - (\sum_{i=1}^{n} u_i)}, \quad (19)$$

$$\alpha = exp\left(\frac{(\sum_{i=1}^{n} w_i)(\sum_{i=1}^{n} u_i^2) - (\sum_{i=1}^{n} u_i)(\sum_{i=1}^{n} u_i w_i)}{-\beta\left(k\sum_{i=1}^{n} u_i^2 - (\sum_{i=1}^{n} u_i)^2\right)}\right). \quad (20)$$

Every failed component need to have a rank assigned in order following the number of cycles passed until failure. Let z_m is the overall rank of the m-th failure and y_m is the adjusted rank of it. Then the adjusted rank for an arbitrary failure will be:

$$y_m = y_{m-1} + \frac{L-1-y_{m-1}}{L+1-(z_m-1)}. \quad (21)$$

With all the ranks set and the median ranks calculated by (17) the estimation of α and β using linear regression provides the ability to find the survival probability and its supplement – the reliability of a given component over the number of cycles used. Survival graphs show the reliability for each design with regards to the number of cycles and direct comparison becomes possible visually.

3 Sensor usage load prediction

In order to evaluate the reliability of a sensor for personal identification capturing human biometrics the typical usage load, that is the number of activation cycles for a given time period, need to be defined. Within this study an attempt is made to estimate the behavior of two types of sensors, described in the next Section, by predicting the frequency of their usage further in time based on the numbers of identifications for known past period.

Suppose the following data set occurs $\{y_i, x_{i1}, \dots, x_{iq}\}_i^n$ from totally of n realizations. Linear approximation of the dependence between y_i and x_{ij} for $j = 1, \dots, q$ could be established [15]. The process includes consideration of the cumulative deviation between the real inputs and the actual result obtained by the approximation denoted by error ε. It is a random value parameter which adds to the general form of the model:

$$y_i = \gamma_0 + \gamma_1 x_{i1} + \cdots + \gamma_q x_{iq+}\varepsilon_i = \vec{x}_i^T\vec{\gamma} + \varepsilon_i, \quad (22)$$

where $i = 1, \dots, n$. For the complete sequence of n observations (22) takes the form:

$$\vec{y} = \vec{x}\vec{\gamma} + \vec{\varepsilon}, \quad (23)$$

where $\vec{y} = (y_1, y_2, \dots, y_n)^T$ is a vector column of the dependent values; $\vec{x} = (\vec{x}_1^T, \vec{x}_2^T, \dots, \vec{x}_n^T)^T$ - vector column of row vectors of the independent values; $\vec{\gamma} = (\gamma_0, \gamma_1, \dots, \gamma_q)^T$ - vector column of parameters defining the linear approximation, totally (q+1) in number; $\vec{\varepsilon} = (\varepsilon_1, \varepsilon_2, \dots, \varepsilon_n)^T$ – vector column of the error parameters.

Equation (22) is also known as linear regression model and it holds stronger when the following conditions are met: weak exogeneity, linearity, constant variance, independence of errors within the dependent variables, that is they are decorrelated, absence of complete muticolinearity while predicting [15].

Fitting a straight line within the distribution of x_i against y_i from all observed realizations i, follows from its analytical expression:

$$y = \gamma x + \delta, \quad (24)$$

where the slope of the line is defined by γ and the crossing with the ordinate – with δ. Proper values for these two parameters are those minimizing the error ε of the approximation. The least-squares approach [15] provides the following solutions for them:

$$\delta = \bar{y} - \gamma\bar{x}, \quad (25)$$

$$\gamma = \frac{\sum_{i=1}^{n}(x_i-\bar{x})(y_i-\bar{y})}{\sum_{i=1}^{n}(x_i-\bar{x})^2}, \quad (26)$$

where the $\bar{x}$ and $\bar{y}$ are the mean values from x_i and y_i respectively.

4 Sensor types for evaluation

4.1 Capacitive fingerprint sensor

Fingerprint recognition systems often use a capacitive type of a sensor. The principle of operation of such biometric stations becomes clear from Fig. 2 silicon integrated circuit acts as a base for the sensor. Covered with metallic plates and protective overlay over them the ridges of the finger with their specific capacitance C_F and the capacitance of the sensor C_S formed to the pads underneath allows charge to accumulate within them. Once registered it becomes the source of forming the image of the fingerprint.

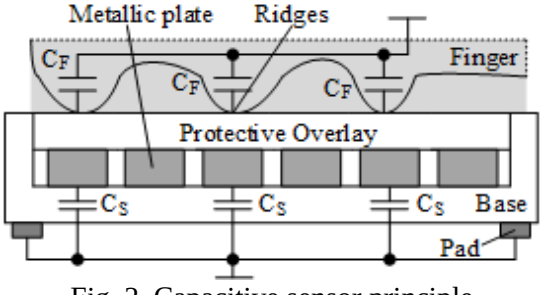

Fig. 2. Capacitive sensor principle

Exemplary model of a sensor that could be used for fingerprinting has life-time of about 10 000 hours [16]. Sensors of this type typically have resolution of 500 dpi with hardness of 8H. The sensing area is around 15x10 mm. Operating temperature covers the range of [20, 60] ºC at humidity less than 90 % and the storage temperature is within the range of [-20, 85] ºC. The power input is most often 5 V DC. The least number of finger placements prior to failure starts at around 2 million for the general production line.

4.2 Optoelectronic fingerprint and finger vein sensor

Fingerprints could be combined with finger veins as previous investigations reveal [12, 17, 18] in multimodal biometrical features leading to higher confidence in personal identification. One single sensor could capture both features using the principle shown in Fig. 3.

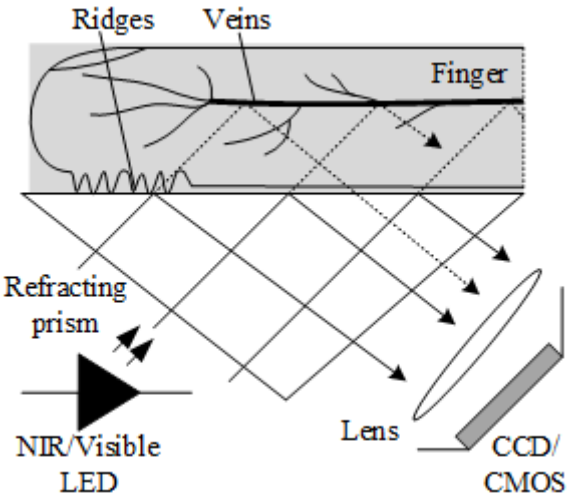

Fig. 3. Optoelectronic sensor for fingerprint and finger vein capturing

Light emitting diode (LED) illuminated the finger with visible and near infrared (NIR) light through refraction prism made of glass. The NIR stream passes through the skin and reflects partially from inner tissue of the finger including veins and becomes modulated by their spatial structure. The visible stream reflects from the surface formed by the ridges of the finger modulating itself to its structure. Both streams are captured by a CCD or CMOS sensors after gathering from appropriate set of lens producing two images from which both features are calculated.

Devices of this type are currently available on the market [19]. They also reach 500 dpi resolution. Their size may cover area up to 7,62 by 8.13 cm which allow multi-finger verification with one scan. The thickness of the sensing part is less than 0.3 mm when produced in flexible design. The latter guarantees conformability, higher sensitivity than capacitive sensors and smaller number of bulky units. Multi-spectral imaging like combining NIR and visible light is easier to implement with them.

The typical life span of a sensor of the type considering only the optoelectronic part is around 100 000 hours [20].

5 Sensors Reliability Evaluation

5.1 Usage cycles testbed

As a real-world example the passenger flow through Sofia airport, Bulgaria, from 2013 to 2018 [21] acts as a base for predicting the future load for the evaluated biometric sensors. The total number of passengers by year is given in Fig. 4.

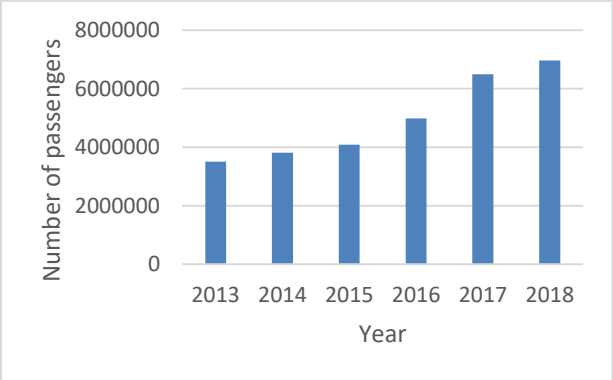

Fig. 4. Passengers flow at Sofia airport

The change of the flow of travelers from year to year is given in Fig. 5.

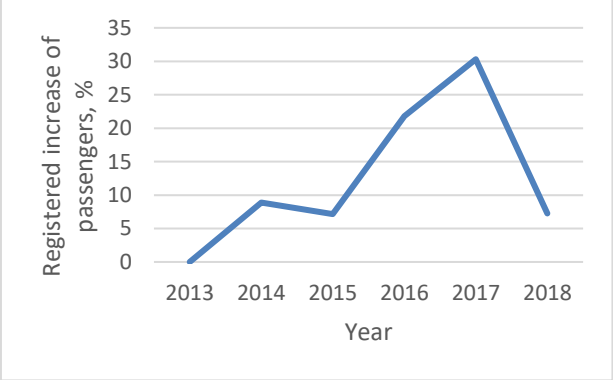

Fig. 5. Number of passengers change

Applying the linear regression approach described in Section 3 the future flow up to 2031 is predicted and shown in Fig. 6. The parameters of the fitting line are: γ = 748722, δ = 7.10^6. The R^2-value of the fitting is close to 1.

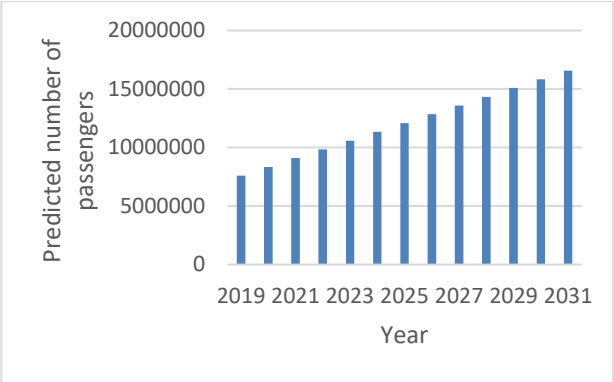

Fig. 6. Predicted flow of travelers at Sofia airport

The change in predicted number of travelers is depicted in Fig. 7.

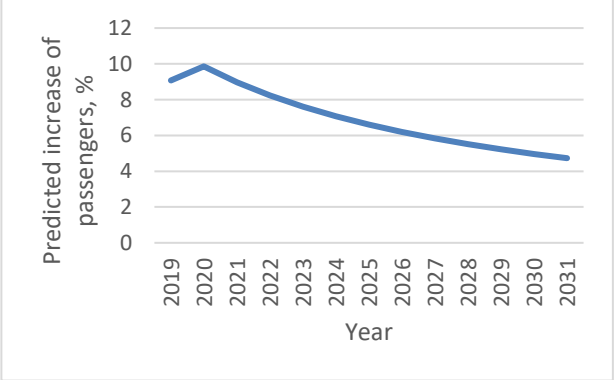

Fig. 7. Predicted travelers number change

The number of cycles until failure for both evaluated sensors for 10 units each are presented in Table 1.

Table 1. Sensors failure data

Sample	Optoelectronic sensor	Capacitive sensor
1	10 523 982	1 038 884
2	13 807 750	1 385 766
3	13 146 179	1 445 775
4	10 965 715	1 597 327
5	11 831 679	1 617 936
6	7 607 990	1 283 014
7	15 528 035	1 180 418
8	18 250 937	1 202 909
9	9 403 728	1 141 568
10	16 610 249	944 272

5.2 Capacitive fingerprint sensor reliability evaluation

Following the methodology described in Section 2 the number of cycles prior to failure for all specimen of the capacitive sensor associate with a rank in ascending order. Then, they are connected with the median ranks and related logarithmic representations from (14). Table 2 includes all found parameter values.

Table 2. Capacitive sensor rank and associate parameters values

Rank	Median Ranks	1/(1-Median Rank)	ln(ln(1/(1-Median Rank)))	ln(Cycles)
1	0,07	1,07	-2,66	13,76
2	0,16	1,20	-1,72	13,85
3	0,26	1,35	-1,20	13,95
4	0,36	1,556	-0,83	13,986
5	0,45	1,82	-0,51	14,00
6	0,55	2,21	-0,23	14,06
7	0,64	2,81	0,03	14,14
8	0,74	3,85	0,30	14,18
9	0,84	6,12	0,59	14,28
10	0,93	14,86	0,99	14,30

Table 3 depicts the results from the linear regression analysis.

Table 3. Capacitive sensor regression analysis statistics

Multiple R	0,982711149
R Square	0,965721202
Adjusted R Square	0,961436352
Standard Error	0,218966159
Observations	10

The analysis of the variance contains all the values given in Table 4.

Table 4. Capacitive sensor analysis of the variance parameters

	df	SS	MS	F	Signifi-cance F
Re-gression	1	10,81	10,81	225,38	3,83 E-07
Residual	8	0,38	0,05		
Total	9	11,19			

The magnitude of α is 1377769,69 and β from the Weibull distribution along with the standard error and other associated parameters are listed in Table 5.

Table 5. Shape parameter and characteristic life of the Weibull distribution for the capacitive sensor

	Intercept	ln(Cycles)
Coefficients	-87,28	6,17 (β)
Standard Error	5,78	0,41
t Stat	-15,10	15,01
P-value	3,66 E-07	3,83 E-07
Lower 95%	-100,61	5,23
Upper 95%	-73,95	7,12
Lower 95,0%	-100,61	5,23
Upper 95,0%	-73,95	7,12

The residual output from finding the Weibull distribution in this case could be seen in Table 6.

Table 6. Residual output from estimating the distribution for the capacitive sensor

Observation	Predicted ln(ln(1/(1-Median Rank)))	Residuals
1	-2,33	-0,33
2	-1,74	0,02
3	-1,16	-0,04
4	-0,95	0,13
5	-0,84	0,33
6	-0,44	0,21
7	0,04	0
8	0,30	0
9	0,91	-0,32
10	0,99	0

Fig. 8 contains the visual representation from the line fitting along with the sample data points.

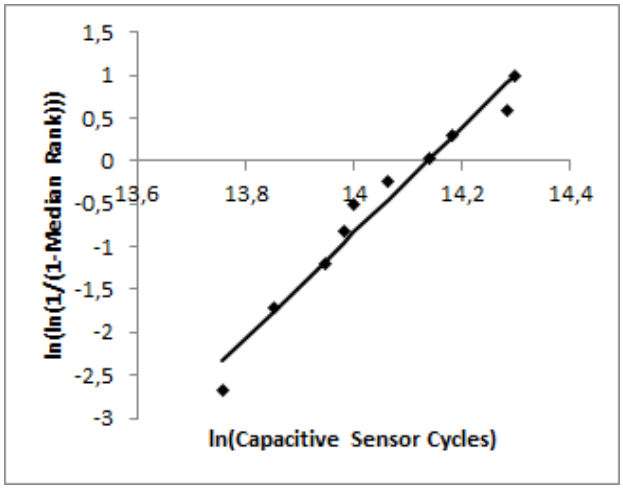

Fig. 8. Line fitting for the capacitive sensor

After establishing the exact type of the Weibull distribution for the capacitive sensor it becomes possible to predict its reliability given a number of cycles of operation (Table 7).

Table 7. Survival probability and reliability of the capacitive sensor

Cycles	Survival probability	Reliability
200 000	0,0000	1,0000
400 000	0,0005	0,9995
600 000	0,0059	0,9941
800 000	0,0343	0,9657
1 000 000	0,1291	0,8709
1 200 000	0,3470	0,6530
1 400 000	0,6684	0,3316
1 600 000	0,9193	0,0807
1 800 000	0,9945	0,0055
2 000 000	1,0000	0,0000

The number of cycles guaranteed statistically by some key reliability values are presented in Table 8.

Table 8. Number of cycles of the capacitive sensor to operate given its reliability

Reliability	Cycles
0,01	1 764 402
0,1	1 577 038
0,5	1 298 364
0,9	956 946
0,99	654 041

5.3 Optoelectronic fingerprint and finger vein sensor reliability evaluation

The associated ranks appear in Table 9.

Table 9. Optoelectronic sensor ranks

Rank	Median Ranks	1/(1-Median Rank)	ln(ln(1/(1-Median Rank)))	ln(Cycles)
1	0,07	1,07	-2,66	15,84
2	0,16	1,20	-1,72	16,06
3	0,26	1,35	-1,20	16,17
4	0,36	1,55	-0,82	16,21
5	0,45	1,82	-0,51	16,29
6	0,55	2,21	-0,23	16,39
7	0,64	2,81	0,03	16,44
8	0,74	3,85	0,30	16,53
9	0,84	6,11	0,59	16,63
10	0,93	14,86	0,99	16,72

Completely the same steps of the methodology described in Section 2 give an overview of the capabilities of the optoelectronic sensor for both fingerprint and finger vein capturing.

Coefficients from the linear regression analysis are contained in Table 10.

Table 10. Optoelectronic sensor regression analysis statistics

Multiple R	0,993524574
R Square	0,98709108
Adjusted R Square	0,985477465
Standard Error	0,134372117
Observations	10

The significance value for the regression, along with statistics for the residual and the total effect from approximation lays in Table 11.

Table 11. Optoelectronic sensor analysis of the variance parameters

	df	SS	MS	F	Signifi-cance F
Re-gression	1	11,05	11,05	611,73	7,63 E-09
Residual	8	0,14	0,02		
Total	9	11,19			

Parameters of the Weibull distribution for this case are given in Table 12. The value of α is 14049968,43.

Table 12. Shape parameter and characteristic life of the Weibull distribution for the optoelectronic sensor

	Intercept	ln(Cycles)
Coefficients	-67,34	4,09 (β)
Standard Error	2,70	0,17
t Stat	-24,92	24,73
P-value	7,18 E-09	7,63 E-09
Lower 95%	-73,57	3,71
Upper 95%	-61,11	4,47
Lower 95,0%	-73,57	3,71
Upper 95,0%	-61,11	4,47

Predicted supplements to the median rank in logarithmic form and the residuals for each observation are ordered in Table 13.

Table 13. Residual output from estimating the distribution for the optoelectronic sensor

Observation	Predicted ln(ln(1/(1-Median Rank)))	Residuals
1	-2,51	-0,15
2	-1,64	-0,08
3	-1,18	-0,02
4	-1,01	0,19
5	-0,70	0,19
6	-0,27	0,04
7	-0,07	0,10
8	0,41	-0,11
9	0,68	-0,09
10	1,07	-0,08

The linear approximation of the scattering of sample points after transforming according to (10)-(14) appears as shown in Fig. 9.

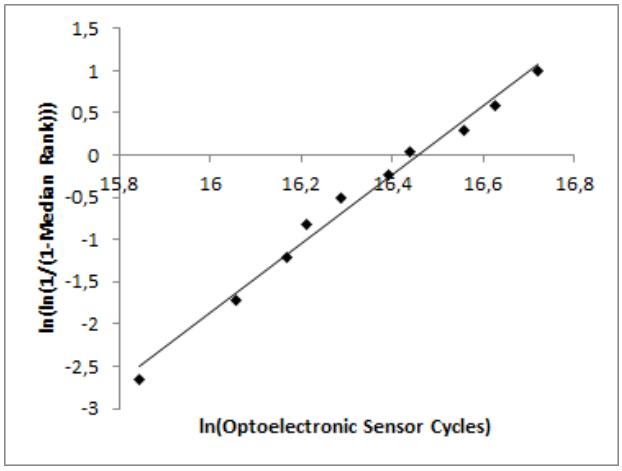

Fig. 9. Line fitting for the optoelectronic sensor

The survival probability and reliability of the optoelectronic sensor at different number of cycles is positioned in Table 14.

Table 14. Survival probability and reliability of the optoelectronic sensor

Cycles	Survival probability	Reliability
2 000 000	0,0003	0,9997
4 000 000	0,0058	0,9942
6 000 000	0,0303	0,9697
8 000 000	0,0950	0,9050
10 000 000	0,2202	0,7798
12 000 000	0,4081	0,5919
14 000 000	0,6268	0,3732
16 000 000	0,8177	0,1823
18 000 000	0,9364	0,0636
20 000 000	0,9856	0,0144

The number of operation cycles expected at various reliability levels are ordered in Table 15.

Table 15. Number of cycles of the optoelectronic sensor to operate given its reliability

Reliability	Cycles
0,01	20 406 405
0,1	17 226 519
0,5	12 846 196
0,9	8 106 377
0,99	4 564 851

5.4 Survival probability comparison of evaluated sensors

Tables 7 and 14 allow to have the survival graphs for both sensors as collocated distributions (Fig. 10).

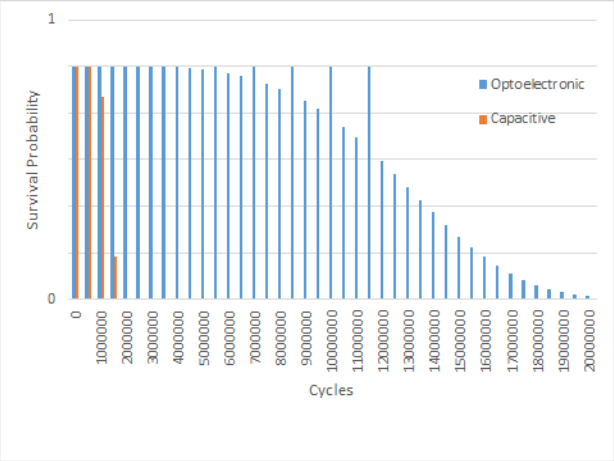

Fig. 10. Survival graphs for both sensors

More detailed view of the survival graph for the capacitive sensor is given in Fig. 11.

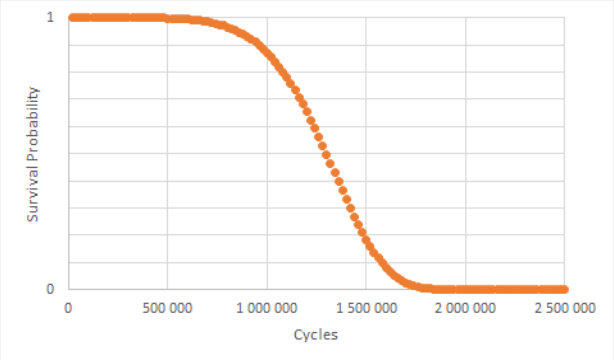

Fig. 11. Survival probability for the capacitive sensor up to 2,5 million cycles

6 Discussion

The failure rate for both sensors is increasing, that is $\beta > 1$, which is expected considering their wearing out over time with processing of the passenger flow. The characteristic life, i.e. α, is quite smaller for the capacitive sensor in comparison to the optoelectronic one – more than 10 times. From a representative population 63.2 % of the capacitive sensors are expected to fail prior to 1,4 Mcycles while the optoelectronic – a bit after 14 Mcycles.

Given the predicted number of travelers for a dozen years (Section 5.1), just 50% of capacitive sensors, supposing that 6 desks are equipped with them, will cover a period close to one year. It means that virtually half of the biometric stations would need substitution of their sensor on annual basis. One tenth of the sensors will continue to operate after three months period afterwards and just 1% will survive close to a 18 month period of exploitation. Ninety percent are going to last at least for 9 months period. With the advancement of time up to 2031 the substitution period will become shorter and shorter taking into account the ever increasing passengers number (Fig. 6).

At the same initial conditions, 50% of the optoelectronic sensors are considered to survive for a period of 7.5 years. Just 1% of them will not require replacement almost to the end of the first decade of their operation. It means that most certainly all biometric stations would have been repaired at least one time up until then. For at least 5 years, 90% of these sensors should survive. Still, 10% will cover around 9 year of capturing.

7 Conclusion

In this paper a detailed prognostic analysis is presented over two types of biometric sensors – optoelectronic and capacitive one. The significant difference in survival probability and the possibility to capture both the fingerprint and finger veins of a person in one scan makes the optoelectronic sensor desirable solution for personal identification. Its technology is currently mature enough and it is widely used in biometric stations for border control. The smaller size, on the other hand, and possible lower cost as well, does not leave the capacitive sensor out of selection, especially in border-crossing points where fingerprints are the only mean for biometric identification.

References:

[1] Ross, A., Jain, A. Biometric Sensor Interoperability: A Case Study in Fingerprints. In the International Workshop on Biometric Authentication, pp. 134-145, Springer, Berlin, Heidelberg, May 2004.

[2] Bahuguna, R., Different Optical Techniques for Sensing of Fingerprints, -International

Conference on Optics and Photonics (ICOP 2009), CSIO, Chandigarh, India, 30 Oct.-1 Nov. 2009, available at http://www.csio.res.in:8080/icop/contents/Saturnday_31.10.09/session%20B3/B3.IT2_R.%20D.%20Bahuguna.pdf , last visited on March 7th, 2019.

[3] Shimamura, T., Morimura, H., Shigematsu, S., Nakanishi, M., & Machida, K. Capacitive-sensing Circuit Technique for Image Quality Improvement on Fingerprint Sensor LSIs. IEEE Journal of Solid-State Circuits, Vol. 45, No.5, pp. 1080-1087, 2010.

[4] Lee, J. W., Min, D. J., Kim, J., Kim, W. A 600-dpi Capacitive Fingerprint Sensor Chip and Image-synthesis Technique. IEEE Journal of Solid-State Circuits, Vol. 34, No. 4, pp. 469-475, 1999.

[5] Tang, H. Y., Lu, Y., Jiang, X., Ng, E. J., Tsai, J. M., Horsley, D. A., & Boser, B. E. 3-D ultrasonic fingerprint sensor-on-a-chip. IEEE Journal of Solid-State Circuits, Vol. 51, No. 11, pp. 2522-2533, 2016.

[6] Han, H., Koshimoto, Y. Characteristics of Thermal-type Fingerprint Sensor. In Biometric Technology for Human Identification V, International Society for Optics and Photonics, Vol. 6944, p. 69440P, March 2008.

[7] Alonso-Fernandez, F., Roli, F., Marcialis, G. L., Fierrez, J., Ortega-Garcia, J., Gonzalez-Rodriguez, J. Performance of Fingerprint Quality Measures Depending on Sensor Technology. Journal of Electronic Imaging, Vol. 17, No. 1, 011008, 2008.

[8] Fingerprints, Biometric Technologies, Whitepaper, January 2017, available at: https://www.fingerprints.com/asset/assets/downloads/fingerprints-biometric-technologies-whitepaper-2017-revb.pdf , last visited on March 7th, 2019.

[9] Hashimoto, J. Finger Vein Authentication Technology and Its Future. In 2006 Symposium on VLSI Circuits, Digest of Technical Papers, pp. 5-8, June 2006.

[10] Raghavendra, R., Raja, K. B., Surbiryala, J., Busch, C. A Low-cost Multimodal Biometric Sensor to Capture Finger Vein and Fingerprint. In IEEE International Joint Conference on Biometrics, pp. 1-7, September 2014.

[11] Yang, L., Yang, G., Yin, Y., Zhou, L. A Survey of Finger Vein Recognition. In Chinese Conference on Biometric Recognition, pp. 234-243, Springer, Cham, November 2014.

[12] Georgiev, D., T. Tashev, I. Draganov, Evaluation of Multimodal Biometrics for Personal Identification based on Score Fusion, In Proc. of the 16th Conference on Challenges in Higher Education and Research in the 21st Century (Cher'21), May 29 - June 1, Sozopol, Bulgaria, pp. 73-80, 2018.

[13] Dodson, B., The Weibull Analysis Handbook, 2 ed., ASQ Quality Press, 2006.

[14] Rinne, H., The Weibull Distribution: A Handbook, Chapman and Hall/CRC, 2008.

[15] Kenney, J., Mathematics of Statistics, 3 ed., Van Nostrand, 1964.

[16] Du, Winncy Y. Resistive, Capacitive, Inductive, and Magnetic Sensor Technologies. CRC Press, 2014, p. 18.

[17] Georgiev, D., T. Tashev, I. Draganov, Biometrics Selection and Their Influence over the Life Cycle of Electronic Identity Documents, WSEAS Transactions on Computers, Vol. 16, pp. 224-233, 2017.

[18] Georgiev, D., T. Tashev, I. Draganov, Investigating the Potential Incorporation of Multimodal Biometrics into Fully Automated Entry-Exit System for the European Union, International Journal of Transportation Systems, Vol. 3, pp. 41-51, 2018.

[19] Flexible Fingerprint Sensors, https://www.flexenable.com/technology/flexible-fingerprint-sensors/, last visited on March 2nd, 2019.

[20] Toal, J., Application of Optical Sensors – Transmissive, Application Note, Vishay, rev. Oct. 25th, 2013, https://www.vishay.com/docs/81449/81449.pdf , last visited on March 2nd, 2019.

[21] Passengers at Sofia Airport, Bulgaria, https://www.sofia-airport.bg/en/business/airlines/statistics/passengers, last visited on February 27th, 2019.